Hindawi
International Journal of Antennas and Propagation
Volume 2022, Article ID 8132254, 7 pages
https://doi.org/10.1155/2022/8132254

Research Article

Structural Design and Electrical Characteristics Analysis of Mid-Load Whip Antenna

Menglei Xiu, Lihua Li, and Shimin Feng

Department of Communication Engineering, Naval University of Engineering, Wuhan 430000, China

Correspondence should be addressed to Shimin Feng; u201812689@hust.edu.cn

Received 5 April 2022; Revised 17 May 2022; Accepted 28 May 2022; Published 14 June 2022

Academic Editor: Shah Nawaz Burokur

In order to facilitate the integration of the offshore surface antenna and reduce the manufacturing cost, the resonance shortening length and omnidirectional radiation performance of a centrally loaded whip antenna are analyzed. By calculating the impedance characteristics of each part of the midload whip antenna, the shortened length of the antenna in the resonance state is obtained; the superimposed field strength of the midload whip antenna to the far field is calculated and its radiation performance is analyzed; the simulation is carried out by using FEKO electromagnetic simulation software. Through the field test, the reflection coefficient and resonant frequency of the antenna before and after shortening are compared, and the directivity of the midload whip antenna and the traditional whip antenna is compared. The simulation and experimental results show that under the preset frequency of 75 MHz, the reflection coefficient of the shortened midload whip antenna decreases by 4.414 dB and 19.09 dB, respectively. The optimal operating frequency is about 68.6 MHz–79.4 MHz, and the bandwidth is 10.8 MHz. Compared with the traditional whip antenna, the midload whip antenna at the radiation null point receives a larger field strength.

1. Introduction

Offshore surface antennas mostly use whip antennas or a combined array of whip antennas. In order to make the whip antenna easy to integrate and reduce the material cost, the physical length of the antenna is reduced based on the resonant length of the ideal monopole antenna, which can effectively solve the problem of antenna miniaturization [1]. At the same time, since the advantage of the whip antenna is that it has omnidirectionality in the horizontal direction, but the radiation performance in the parallel antenna direction has great limitations, so on the premise of realizing the miniaturization of the antenna that increase the omnidirectionality of the antenna in the half space on the sea surface can establish a better communication system to increase reliability [2]. Under normal circumstances, the antenna height of the offshore communication device cannot be very high. To realize the miniaturization of the antenna while keeping the ideal resonant frequency unchanged, the essence is to increase the effective height of the antenna [3]. Adding a top load, although the top load can effectively reduce the physical height of the antenna, the current is almost at the node position. The top load does not directly participate in radiation. In order to improve this situation, the middle loading is appropriately used in this paper [4]. However, in engineering applications, no matter whether the radiator is loaded at the top or the middle, it will affect the current distribution of the antenna and make the antenna deviate from the ideal resonance state [5]. In order to solve this problem, the length of the midload whip antenna needs to be shortened, which can also solve the radiation blind area problem of the traditional whip antenna. In this paper, the structure of the antenna is analyzed and the shortened length of the whip antenna loaded in the middle is quantified, which provides a theoretical basis for the parameter adjustment of the whip antenna in engineering applications [6].

2. Optimization of the Midload Whip Antenna

2.1. Calculation of Resonance Shortening Length. In the case of dealing with the resonance matching of the whip antenna, the top loading method is often used to widen the cross section of the end of the antenna, so as to achieve the effect of miniaturization of the antenna. However, for the whip antenna on the sea surface, it is usually required to have an omnidirectional radiation performance in all directions [7]. At this time, if top loading is adopted, although there is a certain current in the loading part, the current value is small, and it is difficult to achieve omnidirectionality [8]. The purpose of the antenna is that when the middle loading is adopted, the middle loading body of the antenna has a certain energy, which can well compensate for the lack of directivity of the whip antenna [9]. Since the middle loading body separates a part of the current of the top antenna, and the whip antenna itself has a certain radius, it will generate end-face capacitance, so it is necessary to shorten a part of the length of the whip antenna, so that the antenna is in a resonant state at the original frequency.

In order to calculate the effect of the middle loading on the resonant length of the whip antenna, the structure of the antenna needs to be analyzed. Figure 1 shows a schematic diagram of the middle loading whip antenna.

As shown in Figure 1, the antenna is divided into three parts: the first part is the part from the intersection point M of the loading part to the top of the antenna, the length is l_1 and the radius is r_1 and the second part is the part from the intersection point M of the loading part to the feeding point 0, the length is l_2 and the radius is r_1. The third part is the part of the loaded radiator, the length of the radiator is l_0 and the radius is r_0.

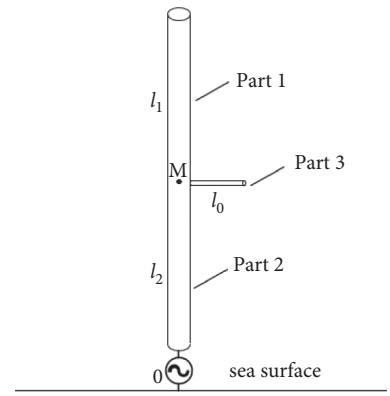

Figure 1: Schematic diagram of the middle loading whip antenna.

First, the input impedance of each part of the antenna should be analyzed.

According to the transmission line theory, it is well known that the characteristic impedance of a uniform dual transmission line is given by [10].

$$Z_0 = 120 \ln \frac{D}{a}, \tag{1}$$

where D is the distance between the uniform double transmission lines and a is the wire radius of the uniform double line. For a symmetric element with a single side length l and a radius a, its input impedance Z_{in} can be regarded as a function of the antenna characteristic impedance Z_0, the antenna radius a, and the antenna single arm length l, that is [11],

$$Z_{\text{in}}(Z_0, a, l) = Z_0 \frac{1}{\text{ch}(2\alpha l) - cos(2\beta l)} \cdot \left[\left(\text{sh}(2\alpha l) - \frac{\alpha}{\beta} sin(2\beta l) - j\left(\frac{\alpha}{\beta} sh(2\alpha l) + sin(2\beta l)\right)\right)\right]. \tag{2}$$

According to the radiation segment theory of the antenna, $\alpha = R/2Z_0$ is the attenuation constant of the antenna, $\beta = 2\pi/\lambda\sqrt{1/2\left[1 + \sqrt{1 + (R\lambda/2\pi Z_0)^2}\right]}$ is the phase shift constant, where $R = 2R_r/l(1 - \sin(2\beta l)/2\beta l)$ and $R_r = 12.35(4\pi/\lambda l)^{2.4}$.

Part 1 of the antenna and its mirror image can be regarded as a lossy uniform double transmission line, so the average characteristic impedance of part 1 of the antenna is as follows:

$$\begin{aligned} Z_{01} &= \frac{1}{l_1}\int_{l_2}^{l_1+l_2} \frac{1}{2} \cdot 120 \ln\left(\frac{2z}{r_1}\right) dz \\ &= 60\left(ln\left(\frac{2(l_1 + l_2)}{r_1}\right) - \frac{l_2}{l_1}\ln\left(\frac{2l_2}{r_1}\right) - 1\right). \end{aligned} \tag{3}$$

Among them, z is the distance from the antenna unit element dz to the feeding point 0. Substituting the average characteristic impedance Z_{01}, wire radius r_1 and antenna length l_1 of part 1 of the antenna into formula (2), the input impedance of part 1 can be obtained as $Z_{\text{in}1}(Z_{01}, r_1, l_1)$.

Similarly, the average characteristic impedance of the antenna part 2 can be obtained, but different from the antenna part 1, its integral range for the antenna is $0 \sim l_2$, which can obtain as follows:

$$Z_{02} = \frac{1}{l_2}\int_{l0}^{l_2} \frac{1}{2} \cdot 120 \ln\left(\frac{2z}{r_1}\right) dz = 60\left(ln\left(\frac{2l_2}{r_1}\right) - 1\right). \tag{4}$$

Similarly, part 3 can be regarded as an elevated monopole antenna, forming a standard uniform dual transmission line with a distance $2l_2$ from its mirrored part, and the average characteristic impedance of the loaded part is as follows:

$$Z_{03} = 60 \ln\left(\frac{2l_2}{r_1}\right). \tag{5}$$

We substitute this into formula (2) as well, and the input impedance of the three parts can be obtained as $Z_{\text{in}3}(Z_{03}, r_0, l_0)$.

The input impedance of point M can be regarded as the parallel connection of part 1 and part 3, the antenna of part 2 can be regarded as a uniform lossy dual transmission line [12], and its termination is connected to the total input impedance $Z_{\text{in},M}$ of point M. The equivalent circuit is shown in Figure 2.

Total input impedance at point M is as follows

$$Z_{\text{in},M} = \frac{Z_{\text{in}3}(Z_{01}, r_1, l_1) \cdot Z_{\text{in}3}(Z_{03}, r_0, l_0)}{Z_{\text{in}3}(Z_{01}, r_1, l_1) + Z_{\text{in}3}(Z_{03}, r_0, l_0)}. \tag{6}$$

At this time, the total input impedance of the antenna at the feeding point 0 can be obtained [13].

$$Z_{\text{in},0} = \frac{Z_{\text{in},M} + Z_{02}\text{th}[(\alpha_2 + j\beta_2)l_2]}{Z_{02} + Z_{\text{in},M}\text{th}[(\alpha_2 + j\beta_2)l_2]}. \tag{7}$$

If the midload antenna is in a resonant state, the reactance part of the antenna needs to be zeroed, that is, the imaginary part of $Z_{\text{in},0}$ is $\text{Im}(Z_{\text{in},0}) = 0$. At this time, the resonance length at the frequency f_0 can be obtained. We explain that when the impedance part $\text{Im}(Z_{\text{in},0}) = 0$ of the total input impedance at the feeding point 0, the length $\Delta l = \lambda_0/4 - l_1 - l_2$ that needs to be shortened can be expressed as $\Delta l = \{\lambda_0/4 - l_1 - l_2 | \text{Im}(Z_{\text{in},0}) = 0\}$; then, this part should be shortened by Δl due to the current and impedance distribution of the antenna.

2.2. Radiation Field Strength Calculation. The polar coordinate system as shown in Figure 3 is established, and the antenna is also divided into part 1, part 2, and part 3.

Part 1 of the antenna is mainly used to adjust the resonant frequency of the antenna, so that the antenna can have a smaller reflection coefficient when it operates at the preset frequency and can also radiate energy together with part 2. Part 3 is mainly used to improve the radiation null problem of whip antenna and increase the omnidirectionality of antenna.

Let the current $I(0)$ at the antenna feed point 0, the current at point M is approximately expressed as follows:

$$I(M) = I(0)\sin\left[\frac{2\pi}{\lambda_0}\left(\frac{\lambda_0}{4} - l_2\right)\right]. \tag{8}$$

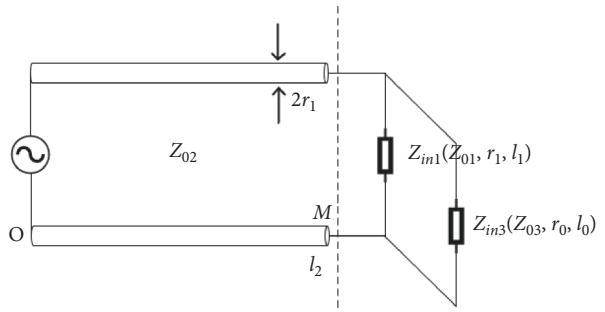

Figure 2: Equivalent circuit diagram of the mid-load whip antenna.

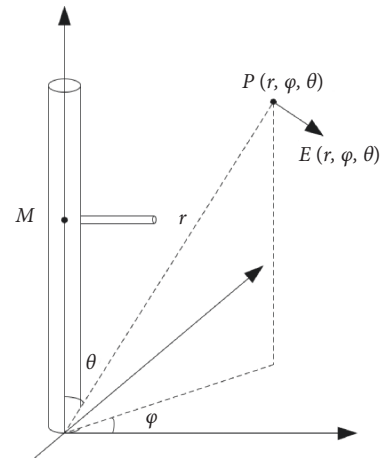

Figure 3: Schematic diagram of far-field radiation of the midload whip antenna.

At this time, the input current of part 1 is as follows:

$$I_1 = \frac{Z_{\text{in}3}(Z_{03}, r_0, l_0)}{Z_{\text{in}1}(Z_{01}, r_1, l_1) + Z_{\text{in}3}(Z_{03}, r_0, l_0)} I(\text{M}). \tag{9}$$

The input current of part 3 is as follows:

$$I_2 = \frac{Z_{\text{in}1}(Z_{01}, r_1, l_1)}{Z_{\text{in}1}(Z_{01}, r_1, l_1) + Z_{\text{in}3}(Z_{03}, r_0, l_0)} I(\text{M}). \tag{10}$$

The field strength contribution of the antenna part 1 to a certain point $P(r, \varphi, \theta)$ in the far field can be approximately calculated as follows:

$$E_1 = j\frac{60I_1}{\lambda_0}\frac{e^{-j2\pi/\lambda_0 r}}{r} \cdot \left(\sin\int_{l_2}^{l_1+l_2} \sin\frac{2\pi}{\lambda_0}(l_1 + l_2 - z)e^{j2\pi/\lambda_0 z\cos\theta}\text{d}z + \sin\int_{-(l_1+l_2)}^{-l2} \sin\frac{2\pi}{\lambda_0}(l_1 + l_2 + z)e^{j2\pi/\lambda_0 z\cos\theta}\text{d}z\right). \tag{11}$$

The field strength contribution of antenna part 2 to this point is as follows:

$$\begin{aligned} E_2 &= j\frac{60I(0)}{\lambda_0}\frac{e^{-j2\pi/\lambda_0 r}}{r} \cdot \sin\int_{-l_2}^{l_2} \sin\frac{2\pi}{\lambda_0}(l_2 - |z|)e^{j2\pi/\lambda_0 z\cos\theta}\text{d}z \\ &= j\frac{60I(0)}{r}\frac{\cos(2\pi/\lambda_0 l_2\cos\theta) - \cos(2\pi/\lambda_0 l_2)}{\sin\theta} \cdot e^{-j2\pi/\lambda_0 r}. \end{aligned} \tag{12}$$

The field strength contribution of antenna part 3 to this point is as follows:

$$E_3 = j\frac{60I_2}{\lambda_0}\frac{e^{-j2\pi/\lambda_0 r}}{r}\cos\theta\int_0^{l_0}\sin\frac{2\pi}{\lambda_0}(l_0-|z|)e^{j2\pi/\lambda_0 z\sin\theta}\mathrm{d}z + \frac{e^{-j2\pi/\lambda_0(r+2l_2)}}{r}\cos\theta\int_0^{l_0}\sin\frac{2\pi}{\lambda_0}\left(l_0-|z|^{j2\pi/\lambda_0(z+2l_2)\sin\theta}\right)e^{j2\pi/\lambda_0 z\cos\theta}\mathrm{d}z. \tag{13}$$

Therefore, it can be concluded that the superimposed field strength of the midload whip antenna to a certain point in the far field is as follows::

$$E(r,\varphi,\theta) = E_1 + E_2 + E_3. \tag{14}$$

The magnitude of the superimposed field strength can effectively reflect the omnidirectionality of the midload whip antenna in the far field and solve the radiation blind area problem of the traditional whip antenna.

3. Simulation

In order to verify the accuracy of the calculation, the resonance length of the midload whip antenna is confirmed. FEKO electromagnetic simulation software is used for simulation calculation. Figure 4 shows a simulation diagram of a midload whip antenna. The antenna adopts a copper conductor, which makes it work at 75 MHz, its radius is 3 mm, and the ideal resonance length is 1 m. The middle loading body is also made of a copper conductor with a radius of 3 mm and a length of 20 cm. Considering that the current distribution of the loading body cannot be too small, and if it is too low, the radiation performance will be lost due to the mirror effect, so it is loaded on the antenna 0.5 m away from the feeding point. We calculate the resonant length of the whip antenna to be shortened and compare the directivity of the centrally loaded whip antenna with the traditional whip antenna. It can be obtained by calculation that if the midload whip antenna is to be in a resonant state, its length should be shortened by $\Delta l = 6.94$ cm. Figure 5 shows a comparison of the reflection coefficients of the shortened and nonshortened midload whip antenna. Because the relationship between the reflection coefficient R_C and the return loss R_L is $R_C(\mathrm{d}B) = -R_L(\mathrm{d}B)$, the energy consumed by the antenna due to the matching problem is equal to the energy reflected from the antenna [14].

It can be seen that when the length of the whip antenna loaded in the middle is not shortened, its resonant frequency is 69.97 MHz, and the reflection coefficient is −12.606 dB. At this time, if it works at the ideal resonant frequency of 75 MHz, its reflection coefficient is about −8 dB. Compared with the reflection coefficient of −12.606 dB, there is a large mismatch loss of about 4.606 dB; when the antenna is shortened by 6.94 cm, the resonance frequency of the antenna rises to 74.52 MHz and the reflection coefficient is −12.417 dB, which is basically equal to the ideal resonance frequency. This shows that shortening the antenna after theoretical calculation can better make the antenna close to the resonance state at the preset frequency and has a smaller reflection coefficient than when the antenna is not shortened. To a certain extent, the correctness of the above calculation derivation is verified.

Figure 6 shows the comparison of the directivity of the midload whip antenna and the traditional whip antenna. Because the pattern of the whip antenna is symmetrical, the XOZ plane $(\varphi = 0^o, 180^o; \theta \in [-90^o, 90^o])$ is intercepted, which is representative.

It can be seen that the closer the traditional whip antenna is to $\theta = 0^o$, the worse its directivity is, and it can hardly work when receiving or transmitting signals. When it is loaded in the middle, the middle loading body radiates energy outward, which can not only maintain the good directivity of the original whip antenna in other directions but also reduce the blind area of the traditional whip antenna to a certain extent. This shows that the directivity of the whip antenna loaded in the middle is better than that of the traditional whip antenna, which is in good agreement with the theoretical derivation.

4. Field Test

In order to better verify the theoretical derivation and simulation results, the shortening effect and radiation performance of the midload antenna will be tested. Figure 7 shows an experimental diagram of the reflection coefficient test of the self-made midload whip antenna. In order to be consistent with the simulation experiments, the radius of the conductor is 3 mm, the preset frequency is 75 MHz, and the initial length of the whip antenna is 1 m, which is the ideal resonance length. The middle loading body has a radius of 3 mm and a length of 20 cm and is loaded at a position 0.5 m away from the antenna feeding point. The bottom of the antenna is placed in the salt water that simulates the seawater environment prepared in the figure, and a network analyzer is used to collect data on the resonant frequency and reflection coefficient of the antenna. First, we measure the parameters of the antenna without shortening, and the measurement results are shown in Figure 8.

It can be seen that its resonant frequency is 67.19 MHz, the reflection coefficient is −25.62 dB, and its reflection coefficient is about −5.35 dB at the preset frequency of 75 MHz. The operating frequency is about 68.6 MHz–79.4 MHz and the bandwidth is 10.8 MHz.

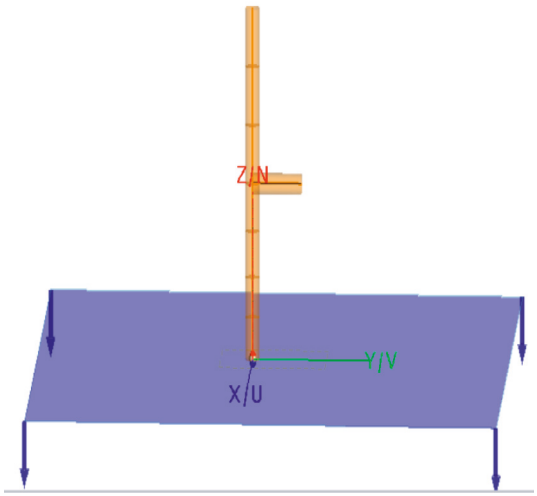

Figure 4: Simulation diagram of the midload whip antenna.

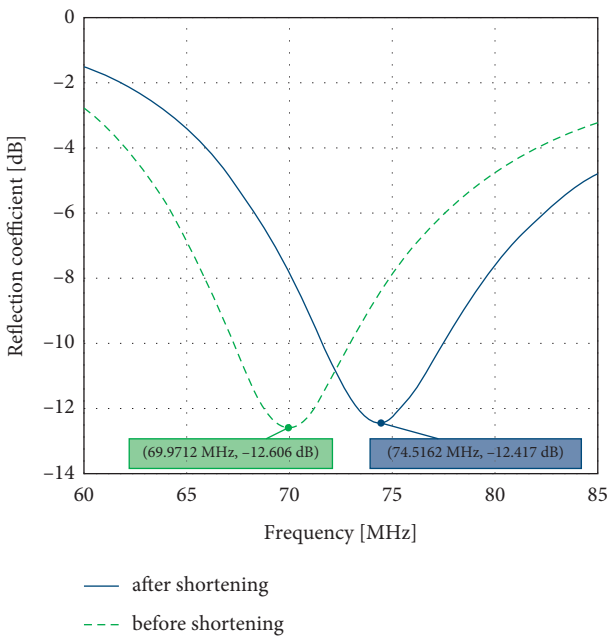

Figure 5: Comparison of reflection coefficients of shortened and nonshortened midload whip antennas.

Then, we test the parameters of the antenna shortened by 6.94 cm, and the measurement results are shown in Figure 9.

It can be seen that its resonant frequency is 74.35 MHz, the reflection coefficient is −26.02 dB, and its reflection coefficient is −24.44 dB at the preset frequency of 75 MHz.

It can be seen from the experimental results that the resonant frequency of the nonshortened midload whip antenna has a large deviation from the ideal resonant frequency, and the reflection coefficient is large at the preset frequency. After the antenna is shortened, the resonant frequency of the antenna gradually approaches the ideal resonant frequency and the reflection coefficient at the preset frequency decreases accordingly. At 75 MHz, the reflection coefficient of the shortened antenna is improved by 19.09 dB

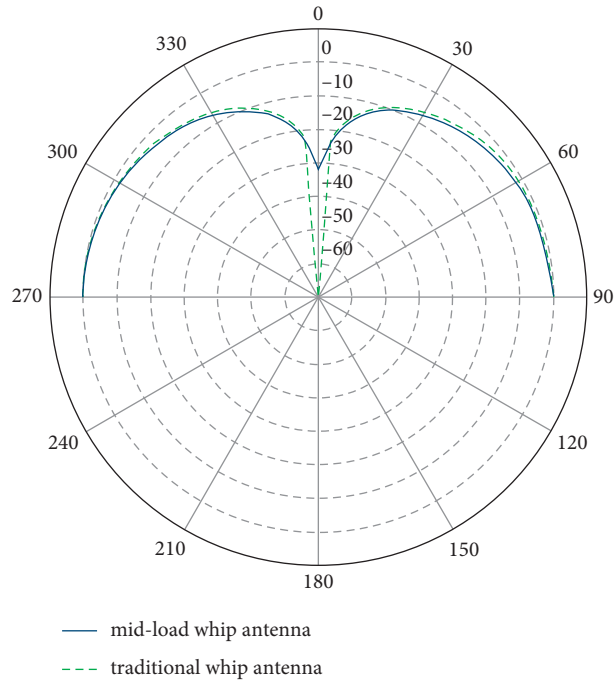

Figure 6: Directivity comparison between the midload whip antenna and the traditional whip antenna.

Figure 7: Experimental diagram of the reflection coefficient test of the self-made midload whip antenna.

compared with the nonshortened antenna. This shows that shortening the antenna to a certain length changes the impedance distribution of the antenna, which is also in high consistency with the theoretical calculation and simulation experiments and further proves the correctness of the derivation process.

The omnidirectional test of the antenna is carried out in the external field, and the test is carried out by loading the

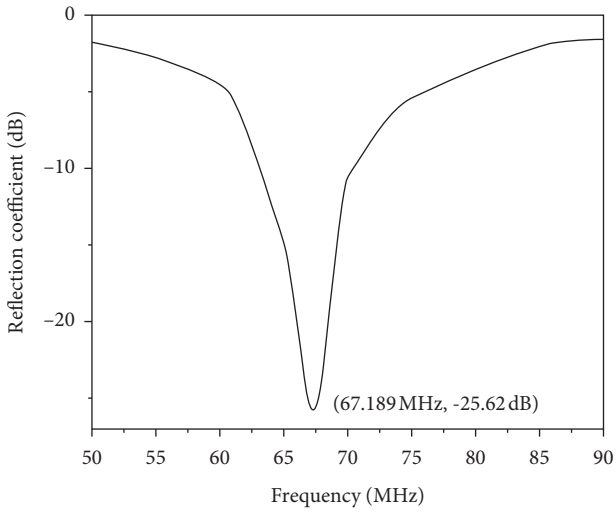

Figure 8: Resonant frequency and reflection coefficient of the midload whip antenna without shortening.

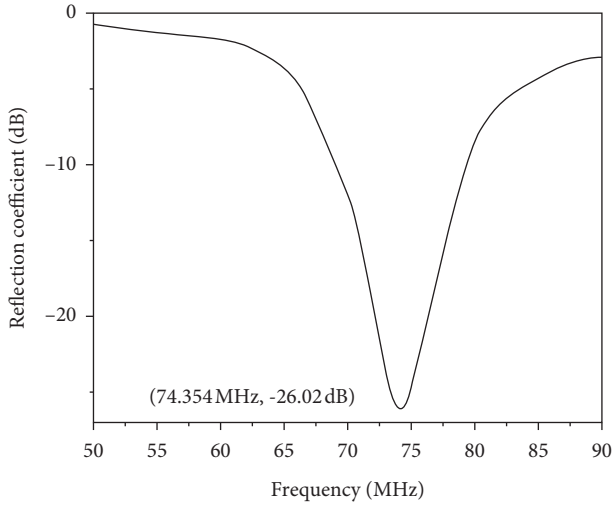

Figure 9: Resonant frequency and reflection coefficient of the midload whip antenna with shortening.

Table 1: Comparison of field strengths received by receivers at different distances.

Distance (meters)	Midload whip antenna (mV/m)	Traditional whip antenna (mV/m)
10	36.14	8.32
20	28.26	6.54
30	17.63	3.21

whip antenna in the middle and the traditional whip antenna in the direction $\theta = 0^o$ (because theoretically, this direction is the radiation blind area of the traditional whip antenna), because the directivity cannot be obtained well. Therefore, the receiving field strength of the far field is used to indirectly prove the radiation capability of the antenna. The directions of 10 m, 20 m, and 30 m were selected for testing. The experimental results are shown in Table 1.

Obviously, the centrally loaded whip antenna solves the radiation blind area problem of the traditional whip antenna. Theoretically, in the blind area, the signal transmitted by the traditional whip antenna should not be received, but the receiver may still receive a very small signal due to the diffraction ability of electromagnetic waves.

5. Conclusions

This paper solves the difference between the ideal resonant length and the actual resonant length of a midload whip antenna at the ideal operating frequency. In engineering, this error is mainly achieved by direct measurement and no literature has disclosed this method to calculate the length of shortening. Second, the middle loading body not only realizes the miniaturization of the whip antenna but also solves the blind area problem of the whip antenna to a certain extent, which is the omnidirectionality especially required for the offshore antenna. The article analyzes the antenna from three aspects: calculation, simulation, and field test. The results all show that the shortening of the midload antenna is beneficial to reduce the reflection coefficient of the antenna, make the antenna resonant frequency closer to the preset frequency, and avoid large energy loss. The simulation and experimental results show that under the preset frequency of 75 MHz, the reflection coefficient of the shortened midload whip antenna decreases by 4.414 dB and 19.09 dB, respectively. Compared with the traditional whip antenna, the simulation gain of the midload whip antenna at the radiation null point is increased to −26.7 dBi. At the same time, it provides a certain omnidirectionality for the whip antenna and provides a theoretical basis for the design and radiation analysis of the offshore surface antenna.

Data Availability

The data of the simulation and experimentation used to support the findings of this study are included within the article.

Conflicts of Interest

The authors declare that they have no conflicts of interest.

Acknowledgments

This work was supported by National Natural Science Foundation of China (41774021, 41874091, and 42074074) and National Natural Science Foundation of China Youth Fund (62101579).

References

[1] Y. Ma and S. He, "A design method of short-wave broadband whip antenna," *Chinese Journal of Radio Science*, vol. 33, no. 3, pp. 365–370, 2018.

[2] H. Wang, C. Liu, X. Xie, and H. Wu, "Gain-improved VHF broadband whip antenna loaded with radiation blades," *IET Microwaves, Antennas & Propagation*, vol. 14, no. 12, pp. 1446–1454, 2020.

[3] H. Wang and C. Liu, "Switchable design of a frequency reconfigurable broadband whip antenna in high frequency," *International Journal of Microwave and Wireless Technologies*, vol. 13, no. 5, pp. 454–462, 2020.

[4] H. Wang, C. Liu, and H. X. Wu, "A novel broadband double whip antenna for very high frequency," *Progress In Electromagnetics Research C*, vol. 99, pp. 209–219, 2020.

[5] J. Han and X. Wang, "Design and analysis of micro-satellite whip antenna rotating disk deployable mechanism," *Science Discovery*, vol. 4, no. 6, pp. 393–397, 2016.

[6] D. K. Park, G. S. Yang, G. R. Jeong, and J. C. S. Kim, "Size reduction of HF whip antenna for ship communication," *The Journal of Korea Navigation Institute*, vol. 16, no. 1, pp. 35–40, 2012.

[7] S. Ponnapalli and F. J. Canora, "Whip antenna design for portable rf systems," *Wireless Data Transmission*, vol. 26, pp. 32–40, 1995.

[8] D. M. O'Brien and D. J. N. Wall, "Radiation from a whip antenna mounted on a sphere," *Journal of Physics D: Applied Physics*, vol. 13, no. 12, pp. 2185–2215, 1980.

[9] W. P. Czerwinski, W. R. Free, and C. W. Stuckey, "A compact tubular chamber for impedance and power testing of VHF whip antennas," *IEEE Transactions on Vehicular Technology*, vol. 21, no. 3, pp. 101–108, 1972.

[10] H. Brueckmann, "Improved wide-band VHF whip antenna," *IEEE Transactions on Vehicular Communications*, vol. 15, no. 2, pp. 25–32, 1966.

[11] J. D. Alden and A. D. Carlson, "Developing a whip antenna for submarine service," *Naval Engineers Journal*, vol. 75, no. 4, pp. 769–774, 1963.

[12] L. F. Sanchez, "Measurement of the radiation patterns of navy shipboard High Frequency (HF) antennas on a large warship," *Measurement*, vol. 74, pp. 200–207, 2015.

[13] M. Xiu, L. Li, S. Feng, and W. L. Hou, "Analysis of UUV whip antenna radiated power and optimal working frequency in seawater environment," *Progress In Electromagnetics Research C*, vol. 118, pp. 61–70, 2022.

[14] A. Dharmarajan, P. Kumar, and T. Afullo, "A high gain UWB human face shaped MIMO microstrip printed antenna with high isolation," *Multimedia Tools and Applications*, vol. 607, pp. 873–880, 2022.